LAWRENCE
LIVERMORE
NATIONAL
LABORATORY

LLNL-JRNL-869342

Impact of Mechanical Tolerances on Partial Turn Skipping in Helical Flux Compression Generators

K. Schriner, N. Fryar, T. Watson, J. Stephens, J. Dickens, A. Young, A. Neuber

September 14, 2024

American Institute of Physics Advances

Disclaimer

This document was prepared as an account of work sponsored by an agency of the United States government. Neither the United States government nor Lawrence Livermore National Security, LLC, nor any of their employees makes any warranty, expressed or implied, or assumes any legal liability or responsibility for the accuracy, completeness, or usefulness of any information, apparatus, product, or process disclosed, or represents that its use would not infringe privately owned rights. Reference herein to any specific commercial product, process, or service by trade name, trademark, manufacturer, or otherwise does not necessarily constitute or imply its endorsement, recommendation, or favoring by the United States government or Lawrence Livermore National Security, LLC. The views and opinions of authors expressed herein do not necessarily state or reflect those of the United States government or Lawrence Livermore National Security, LLC, and shall not be used for advertising or product endorsement purposes.

Impact of Mechanical Tolerances on Partial Turn Skipping in Helical Flux Compression Generator

K. Schriner[1], N. Fryar[1], T. Watson[1], J. Stephens[1], J. Dickens[1], A. Young[2], and A. Neuber[1]
[1)] *Texas Tech University, 2500 Broadway W, Lubbock, TX 79409*
[2)] *Lawrence Livermore National Laboratory, 7000 East Ave, Livermore, CA 94550*

(*Electronic mail: Kirk.Schriner@ttu.edu)

(Dated: 14 October 2024)

Maintaining tight mechanical tolerances of the components used in helical flux compression generators (HFCG) is crucial for optimizing device performance. Moving beyond current literature, which provides various approximations for acceptable tolerances, a 3D simulation of the armature stator interaction during generator operation was developed, revealing that existing equations frequently misestimate the tolerance limits. Without restricting the generality of the presented approach, the focus was primarily on the armature's concentricity and roundness, comparing the acceptable tolerance limits between generators of different sizes. An analytical approach for select geometries was developed, confirming the 3D results. Quantitative results reveal that a steeper Gurney angle and increased winding pitch allow for less restrictive tolerances for eccentricity and ellipticity. Even small deviations from the ideal armature positioning and shape will result in fluctuations of the output current time-derivative, observed experimentally and in simulation. Larger deviations then cause partial turn skipping, associated with loss of magnetic flux. The simulation elucidates the impact of tolerance deviations on generator performance by offering precise tolerance ranges for various generator sizes, thereby facilitating informed design decisions.

I. INTRODUCTION

Achieving high gain in helical flux compression generators (HFCGs) can be difficult to accomplish due to losses inherent in the generator design. An important measure when discussing gain in HFCGs is flux conservation, which is the ratio of the initial total magnetic flux (Φ_0) to the final total magnetic flux (Φ_f) found in the generator, or Φ_f/Φ_0.[1] A conservation ratio closer to unity equates to a generator which performs closer to the lossless, ideal design.

In an ideal HFCG, when the armature contacts the stator windings, the contact point between armature and stator smoothly propagates along the helix path. When tolerance issues are present in HFCG construction, causing misalignment between the armature and stator, the contact point propagation can become discontinuous, skipping some fraction of a stator helix turn. This results in a portion of flux that becomes trapped behind the contact point and, therefore, is not compressed, resulting in an overall lower flux conservation ratio. This is often referred to as "turn-skipping" and is a cause of poor generator performance.[2] Armature-stator misalignment, out-of-round armatures, and inconsistent wall thicknesses are all primary contributors to flux loss through turn-skipping, degrading the generator's performance.[3, 4]

If the mechanical tolerances are such that the effect repeats itself with every stator turn, it is known as "2π clocking" and manifests as some modulation/loss in the *dI/dt* output of the HFCG. To this effect, these losses appear at a constant rate, determined by the pitch, and at exactly 360°, or 2π radians away from each other.[21] This phenomenon is addressed in more detail in Results Section E.

Several HFCG design variables dictate the minimum mechanical tolerances required for preventing turn-skipping. As will be shown in the analysis to come, the stator windings' pitch and the expansion angle of the armature, also known as the Gurney angle[16], are two of the critical parameters determining the minimum tolerances required to prevent turn-skipping. Estimate equations are frequently employed to ascertain the minimum tolerances required to avoid turn-skipping in HFCGs. These equations typically provide a single tolerance value, omitting additional information that could be beneficial for the FCG designer. One source of uncertainty stems from the fact that multiple estimate equations exist, which as will be seen provide different tolerances specifications for a single set of design parameters. Thus, it is unclear how HFCG performance may be affected when choosing from the range of tolerance values resulting from the equations. To address this uncertainty, a novel 3D simulation of the armature-stator interaction was developed. The simulation quantifies the effects of tolerance variations on turn-skipping, from the standpoint of elucidating exactly what fraction of a single turn will be skipped for a given tolerance variation. Here, the simulation was used to eliminate any uncertainty from the common estimate equations, for the case of armature-stator radial eccentricity. In this respect, the added value of this new modeling approach is clear – it better enables FCG designers to make tolerance specifications based on unambiguous calculations.

Naturally, practical FCGs will be influenced by the cumulative impact of various tolerance deviations. The combined effects of these deviations on contact point propagation can become highly complex, making it impractical to derive a closed-form solution for estimating resultant turn-skipping. By utilizing a calculated or estimated armature expansion profile, the presented modeling approach identifies potential turn-skipping resultant from multi-modal tolerance variations – a capability yet to be described in the open literature, to the authors' knowledge. In this manuscript, we

demonstrate this capability by analysis of an out-of-round (i.e. suffering from ellipticity) armature.

The simulation model for testing the effects of tolerance variations in HFCGs leverages the physics and collision detection capabilities of Blender™. Modeling the generator in Blender™ 4.0 enables easy characterization and comparison of manufacturing parameters. This paper analyzes turn-skipping as a parameter rather than quantifying flux loss or performance metrics, as compared to other papers that have been published.[2-4] Analyzing the azimuthal angle skipped on a stator winding mimics the real-world behavior of an HFCG. The model allows for fast simulation speed, with, after some optimization, single simulation run times of ~20 minutes were possible on a PC with an Intel Core i7, 8 total cores, 4.80 GHz processor and 32 GB, 3000 MHz DDR4 ram. This allowed for multiple parameter variations and parameter sweeps of the parameter space in which turn-skipping occurs.

Previous research has shown that three main mechanical parameters contribute to partial turn-skipping: the stator winding pitch, armature and stator eccentricity, and armature wall thickness and thickness uniformity. [3] In the presented simulation, a direct correlation between the pitch of the windings and the maximum allowable tolerance is readily characterized. Previous equations provide similar insight, as discussed later in this manuscript. Secondly, the relative eccentricity of the armature and stator is directly proportional to the leading-edge contact point skipping to higher parts of the stator windings. Based on the geometry of the armature expansion, any eccentricity misalignment causes the region of contact between the armature and stator to shift. This shift determines the fraction of the turn skipped.

The third and final influential parameter is the armature wall thickness and thickness uniformity. This is difficult to translate to the scope of our simulation. However, literature shows that these variations cause variations in the ellipticity of the armature as well as alterations in the expansion angle or the Gurney angle. [3] This is accounted for in the model by a change in the Gurney angle and by controlling the direct ellipticity of the starting armature tube.

Note, previous literature has commented on the existence of turn skipping and has derived equations which can be utilized to find the minimum tolerance requirements for HFCGs before turn skipping occurs.[21] The methodology outlined in this paper validates previously established equations and methods by employing innovative techniques and simulations, thereby enhancing earlier results. This paper also elaborates on the manifestation of "2π clocking" in the output *dI/dt* waveforms of generators with high tolerance, a topic that, to the authors' knowledge, has not been previously published.

II. Model Description

Blender™ [23] was selected for its effective collision detection and the capability to directly control the simulation environment using native Python[24]. Python's straightforwardness and Blender™'s user-friendly nature provided a significant advantage over more complex simulation environments, resulting in faster development times compared to starting with a more advanced platform.

The simulation consists of two main bodies: the armature tube and the stator windings. To simulate and detect collisions, the stator winding is modeled by discrete points spaced 0.5° apart over the 0 - 360° azimuthal range, see Fig. 1. These points follow the stator winding structure, maintaining pitch, size, and geometry, which are part of the stator construction. To measure if turn-skipping occurs, each point is numbered, beginning with the first point and ending with the last. If the armature does not contact the points sequentially, turn-skipping has occurred, and the fraction of the turn which has been skipped is determined by the number of points missed in the sequence.

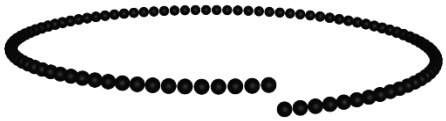

FIG. 1. Visualization of the stator coil in Blender™. (Note that in the simulation, the modeled stator coil uses 720 angle points over the 0-360° azimuthal range.)

A portion of the armature was created, with control over the size, Gurney angle, location, and ellipticity. Only a small portion of the armature was used to optimize the simulation. This armature portion, represented as a truncated cone, retains the essential information about the armature, the Gurney angle, and desired tolerance parameter variations. Hence, faster simulation processing is achieved by excluding unnecessary armature portions. In Fig. 2, the truncated cone is depicted as a portion of the overall armature. The expansion ratio and the Gurney angle are maintained, while the portions of the armature that are not in direct contact with the stator are removed.

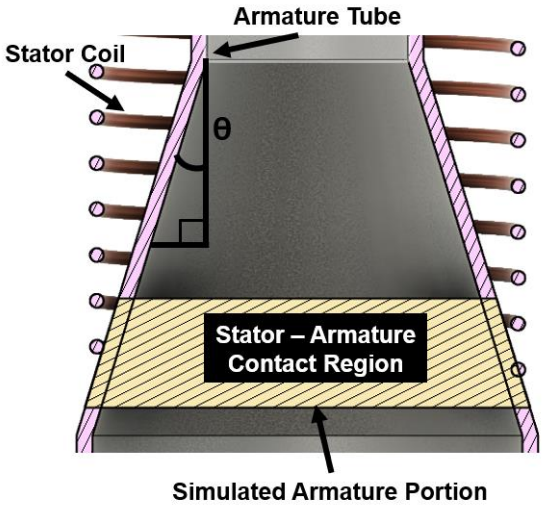

FIG. 2. Cutaway view of modeled armature portion comparison. This consists of a stator coil with a pitch of 2.5 mm. The Gurney angle, θ, here chosen as 17°, is the angle at which the internal armature expands. The portion of the armature that contacts the stator in one instant is highlighted, of which one 360° azimuthal range is modeled in Blender™.

Blender's native framing and collision detection abilities were used to model the interaction between these two bodies.

The stator coil is defined as stationary, while the truncated cone carries all mechanical tolerance defects defined by the user. At a user-defined axial resolution, the simulation incrementally moves the truncated cone upward. After each increment, the simulation checks for any contact between the stator windings and the armature. Referring to the numbered points of the stator windings, see Fig. 1, the model checks where contact has been made and if any part of the winding was skipped.

III. Results

A. Eccentricity Simulation

In the context of a HFCG, the central armature tube is placed concentrically within the stator windings. Eccentricity measures the perpendicular distance between the armature's center axis and the stator windings' center axis, see Fig. 3. When the armature is perfectly centered within the stator, the eccentricity is zero (i.e. perfectly concentric). If the armature and stator geometric centers are mechanically misaligned, then they are eccentric, which, depending on the severity of the misalignment, will result in turn-skipping. In the simulation, when severe enough eccentricity exists between the armature and stator, the progressing contact between the two will skip some of the stator points, thus missing some angular extent of the stator windings. The number of points missed, multiplied by the model resolution (0.5 degrees) provides the metric of "angle skipped," utilized in the following discussion and graphs.

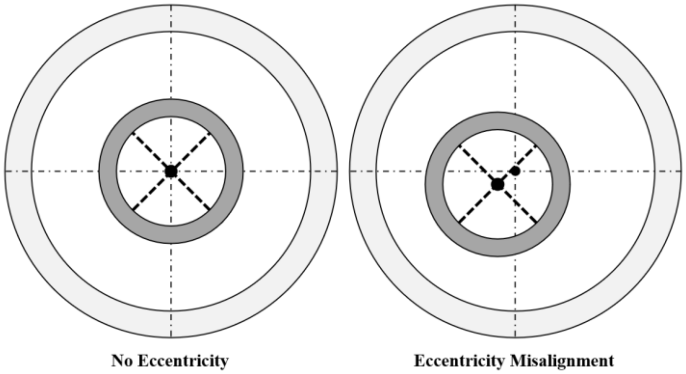

FIG. 3. Graphical depiction of (left) concentric alignment and (right) eccentric alignment between the armature and stator coil. The stator is represented by the outer circle, with the inner, darker circle, representing the armature.

Equations from the literature utilize two parameters to calculate the eccentricity tolerance required before turn-skipping occurs. Some equations that are commonly used are:

$$\Delta a < \frac{P}{4}\tan(\theta) \quad (1)$$

$$\Delta a < \frac{P}{2\pi}\tan(\theta) \quad (2)$$

$$\Delta a < \frac{P}{2}\tan(\theta) \quad (3)$$

where P is the pitch of the stator windings, θ is the armature Gurney angle, and the output, Δa, is the required tolerance to prevent turn-skipping relative to eccentricity. [2-4, 6-7, 19-20] In the simulated scenario, as the degree of eccentricity between the armature and stator increases, a sudden sharp increase in the angle skipped is observed, see Fig. 4. In the same figure, the calculated minimum tolerance values from the equations listed above are compared to the Blender results.

It should be noted that the developed Blender™ simulation was limited to a maximum angle skipped of ~175° due to only considering a single turn of the stator. When considering the full HFCG, it is obvious that the theoretical maximum skip could be much greater than the simulated maximum of ~175°. However, the thrust of this research is to focus on tolerances close to the skipping threshold, and the limit to ~175° is accepted. Changing the offset direction provided the same results regarding the onset of turn-skipping and the slope, but the maximum amount of turn skipped in the simulation may differ since only a single turn is considered.

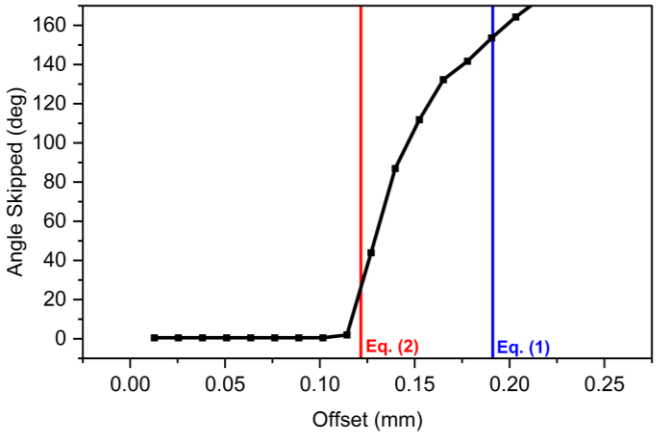

FIG. 4. Comparative tolerance analysis for 17° gurney angle and 2.5 mm pitch. Compares simulation results with equations (1) – (2). Equation (3) had an output value of 0.366 mm and is off-scale.

As shown in Fig. 4, the simulation shows that equation (1) is not conservative enough in predicting the eccentricity tolerance requirements required to prevent the onset of turn-skipping. Moreover, the simulation shows that at the offset value of eccentricity Eq. 1 predicts for the onset of turn-skipping, one would expect ~150 degrees of a 360-degree single stator winding to be skipped, which is approaching half a full turn! Thus, in terms of the onset of angle/turn-skipping, Eq. (2), being the most conservative, yields, in comparison, the most favorable result of the equations listed.

Equation (2) has generally been recognized as the most accurate among the presented equations, as corroborated by the results depicted in Fig. 4. This aligns with findings from various papers on the subject[19-20] and supports the validity of the new simulation method for determining HFCG tolerances.

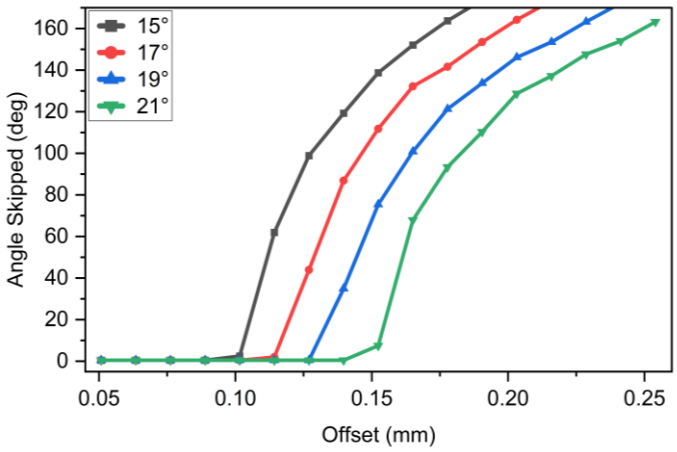

FIG. 5. Plot showing the Gurney angle effect on the onset and severity of turn-skipping. Steeper Gurney angles enable less restrictive tolerances. All simulations were probed with 2.5 mm constant pitch.

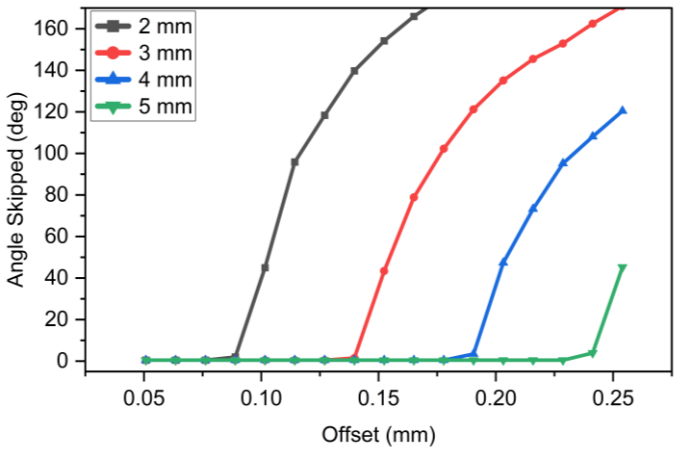

FIG. 6. Plot showing the effect of pitch change on the onset and severity of turn-skipping. A higher pitch enables less restrictive eccentricity tolerances. All simulations assumed a Gurney angle of 17°.

A clear correlation exists between the steepness of the Gurney angle and the effect the eccentricity of the armature and stator have on turn skipping. Both Eq. (2) and the simulation, see Fig. 5, reveal that a steeper Gurney angle enables less restrictive eccentricity tolerance to prevent turn-skipping. Not immediately obvious from inspection of Eqs. 1-3, but clearly evident from the simulation results shown in Fig. 5, is that there's about a 1:1 effect on allowable eccentricity from the Gurney angle. That is, for every 1% increase in the Gurney angle, there's about a 1% increase in allowable eccentricity, for a fixed winding pitch. While maximizing the Gurney angle is attractive with respect to eccentricity tolerances, there are limits to what one can physically realize. In practice, Gurney angle is maximized by maximizing the explosive mass-to-armature mass ratio (in favor of the explosive mass), and by maximizing the energy density of the explosive used. For a given explosive chemistry, tailoring the mass ratio requires thinning of the armature wall, which will be limited by the tendency of the armature to break apart before contacting the stator windings.[9] Advanced high explosive formulations with a higher Chapman Jouguet pressure would enable a steeper Gurney angle, while retaining armature wall thickness[5, 14], although it should be noted that the explosives commonly employed in HFCGs (C-4, PBXN-110, PBX-9501, e.g.) are already among the most energy dense explosives available. Gurney angles of up to 20 degrees have been demonstrated feasible in practice, with documentation showing experimental implementations in the range of 15-20 degrees.[22]

Figure 6 illustrates the relationship between adjusting the pitch and the onset, and severity, of turn-skipping. Similar to the results of the Gurney angle sweep, and more obvious from inspection of Eqs. 1-3, increasing the winding pitch also provides about a 1:1 benefit for allowable eccentricity tolerance.

Neglecting generator gain for the moment, an HFCG with a larger pitch and a larger Gurney angle will be less prone to turn-skipping, enabling less rigid eccentricity tolerances of the armature and stator. Practical FCG designers cannot neglect gain, of course, but we note that the increase in size of a HFCG - for a fixed initial inductance value – will provide opportunity for increased pitch and more relaxed eccentricity tolerances. This idea, and its tradeoffs, are explored in more detail in a subsequent section.

B. Eccentricity-Geometrical Considerations

In a concentric armature-stator alignment, the expanded armature's leading contact edge forms a plane in the stator's frame of reference, with r and θ components only (in cylindrical coordinates). When an eccentric offset is present between the armature and stator, this plane becomes "tilted" in the same frame of reference, and thus also contains a z component as well. Projected into a 2D cartesian coordinate system, see Fig. 7, the plane becomes a line which intersects the stator "boundary" at different vertical (longitudinal) locations. Hence, a high and a low point of armature-stator contact will be created, in the 2D projection.

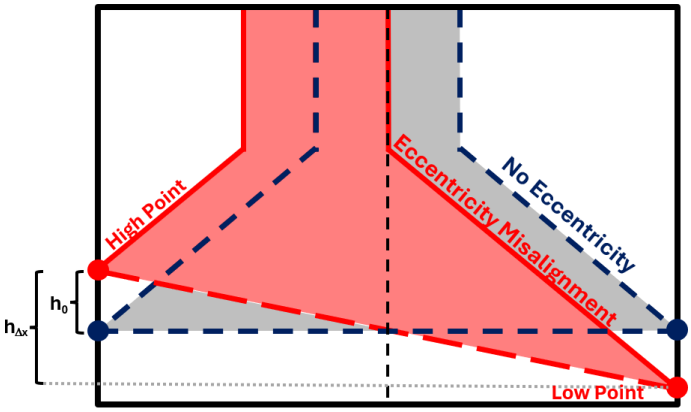

FIG. 7. Eccentric offset 2D plane view of an expanding armature. The border can be considered the stator or the point at which the armature needs to expand. Any offset variation in eccentricity causes a low and high point to develop in the stator-armature contact region.

It is straightforward to evaluate the low and high point difference through geometric relationships, and we find:

$$h_0 = \frac{r_s - r_a}{\tan(\theta)} \tag{4}$$

With h_0 representing the height of the armature tube required to expand from its initial radius, r_a, at the desired Gurney angle, θ, to the stator radius, r_s. Introducing the offset, Δx, yields the difference between the lowest and highest contact point of the armature and stator:

$$h_{\Delta x} = 2\left(\frac{r_s - r_a}{\tan(\theta)} - \frac{r_s - (r_a + \Delta x)}{\tan(\theta)}\right) \tag{5}$$

Noting that the offset is of opposite sign for the low and high points, yields for the height difference between the two:

$$h_{\Delta x} = \frac{2\Delta x}{\tan(\theta)} \tag{6}$$

When no eccentricity is present, the armature expands evenly on all sides and contacts the stator, following the helical path determined by the FCG winding. When projected on a plane normal to the HFCG longitudinal axis, this will result in a circular contact point path. When eccentricity offsets are introduced, the projection plane in which the contact point makes a circular path will become oblique by an angle, ϕ. Setting the intersection between the stator and this oblique plane at its lowest point to zero, the height at any intersection point is found to be periodic and can be described using a sinusoidal function:

$$H(\phi) = \frac{h_{\Delta x}}{2}(1 - \cos(\phi)) \tag{7}$$

This equation utilizes the maximum height of the offset and the sinusoidal characteristics to quantify the contact region of an offset armature. Combining equations 6 and 7 yields the difference in height for any armature offset:

$$H(\phi) = \frac{\Delta x}{\tan(\theta)}(1 - \cos(\phi)) \tag{8}$$

The graphical representation of Equation (8) for an offset of 0.15 mm is depicted in Fig. 8, along with the linear change in helix height due to the pitch as the azimuthal angle progresses in time. Since the line intersects the offset-height in two points, turn-skipping has occurred, and the length of helix wire between these two points is skipped.

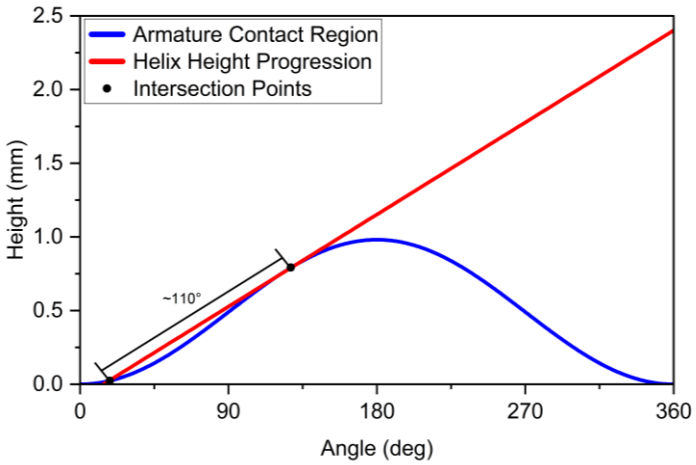

FIG. 8. Graphical representation of armature-stator contact region interaction, showing the height of both the armature and stator contact regions respectfully as a function of angle. Representing an HFCG with a Gurney angle of 17° and a pitch of 2.5 mm. The total angle skipped is 110° for an offset of 0.15 mm.

Comparing calculations from the derived analytic solution for eccentricity-driven turn-skipping with the Blender™ simulation shows exact agreement. Thus, for turn-skipping driven solely by armature-stator eccentricity, the need for estimate equations has been eliminated, and one can determine, with precision, the allowable eccentricity tolerances for a generator design, using only the derived solution. Also note that the geometry-based approach allows for two or more turns to be analyzed, enabling larger offsets to be assessed. For a 0.25 mm offset on the generator depicted above in Fig. 8, the Blender™ simulation, in its current instantiation, would be limited to ~180° (since, as discussed, only a single turn is considered), but based on Eq. (8), 207° would be skipped under these conditions, see Fig. 9. Of course, the Blender™ model is easily extendable to multiple turns and sections.

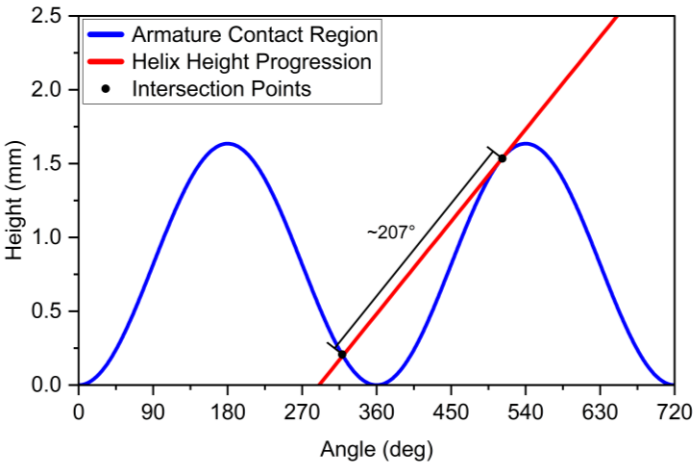

FIG. 9. Graphical representation of armature-stator contact region interaction. Gurney angle of 17°, pitch of 2.5 mm, and an offset of 0.15 mm. The total angle skipped is 207°.

The presented approach mirrors the geometric approach developed by Herlach.[19] While the results are, as expected,

similar, the technique employed here is more modern and capable of analyzing multiple geometries more efficiently. The MATLAB implementation provides a robust geometric simulation that extends the work outlined by Herlach and validates the accuracy of the Blender™ approach.

C. Eccentricity Normalization Results

To simplify the analysis and enhance the readability of the graphs created in Blender™, the variables of pitch and eccentricity are normalized on the tolerance axis of a single graph. This results in a consolidated graph displaying the relationship between the angle skipped and a normalized tolerance. This, in turn, provides a simple reference, from which allowable eccentricity tolerances for any generator design can be calculated.

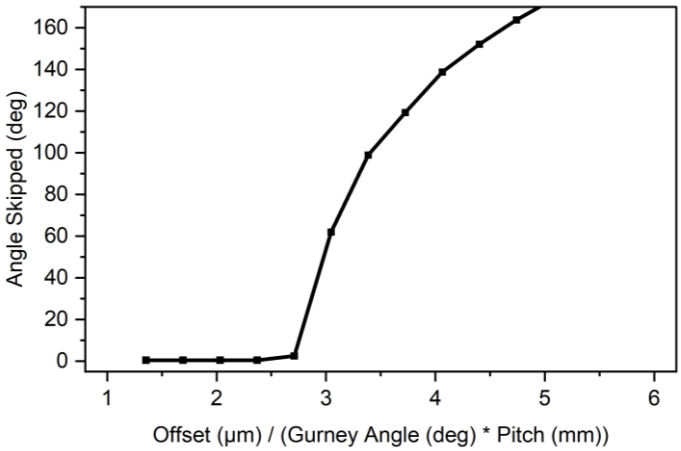

FIG. 10. Shows plot of angle skipped as a function of offset, normalized to gurney angle and pitch, for armature-stator eccentricity.

The normalization graph found in Figure 10 shows the point at which turn skipping occurs is approximately the product of the pitch, in mm, and the Gurney angle, in degrees, multiplied by 2.75. For a specific set of design parameters, one simply needs to scale this "universal" curve by the Gurney angle and pitch to obtain a curve specific to those parameters, see Fig. 11.

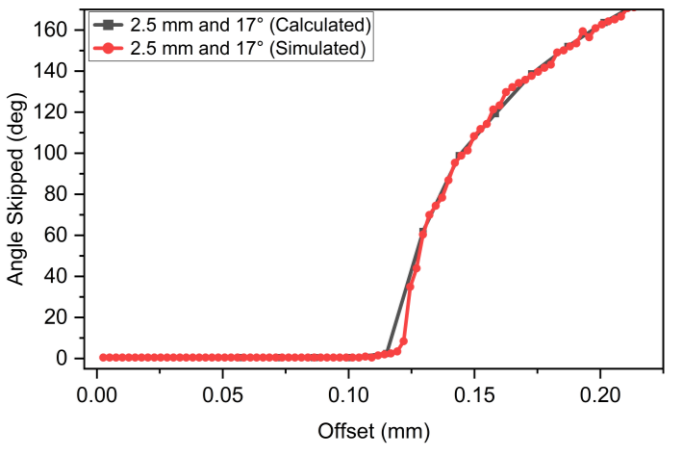

FIG. 11. Blender eccentricity results compared to calculated results using normalized plots from Figure 10, calculated with 17° Gurney angle and a pitch of 2.5 mm.

D. Tolerance Scaling

Tolerance scaling relative to generators is a common discussion point. Historical data suggests that the flux conservation ratio achieved in smaller HFCGs tends to be lower than that of larger ones. A HFCG with the exact same pitch and Gurney angles, no matter the size, will require the same tolerance specifications, with respect to turn-skipping. The inherent advantage in larger generators is that they tend to utilize a larger overall pitch, which allows for less restrictive eccentricity tolerances when compared to a generator of a smaller size.

As an example, if a generator's physical size were to be changed while maintaining a constant inductance, the required tolerances would change. Equations (1) – (3), as well as the normalized graphs above, show the relationship to be a function of the starting pitch divided by the new pitch. Below, in Fig. 12, a specific example is provided for a large and a small generator with the same inductance. Assuming a desired 100 μH inductance, consider an initial design point with a stator radius of 50.8 mm, a length of 300 mm, and an armature with a radius of 25.4 mm. In this case, the simple solenoid equation[18] yields comparable results for the inductance to Olshausen's formulas [13]; both show that an approximately 63 turns is required (67, calculated using Olshausen's), resulting in a stator pitch of 4.76 mm (4.46 mm). If the radial and axial dimensions of the generator are halved while maintaining the desired 100 μH self-inductance, the pitch needs to be adjusted to 1.68 mm (1.58 mm), along with the required number of turns to 89 (95 turns using Olshausen's). The resulting difference in eccentricity tolerance threshold is the ratio of the initial pitch divided by the new pitch, about 0.21 mm to 0.075 mm, cf. Fig. 12. This example illustrates the mechanical challenge of making small HFCGs – a 0.5X scaling of the dimensions results in almost a 3X increase in the required mechanical accuracy. Assuming these values, the amount of angle skipped will be the same. However, it should be noted that the flux loss for a single skip may differ for generators of different sizes. A 60° skip for the smaller pitched generator will lose less flux than the same angle skipped on a larger pitch due to the volumetric difference in the total skipped amount.

It's important to note that although larger generators provide better tolerance and efficiency, they are not always the ideal solution for every application. Some applications exist that necessitate the use of smaller HFCGs, making it crucial to optimize tolerance-dependent parameters to develop an efficient generator.

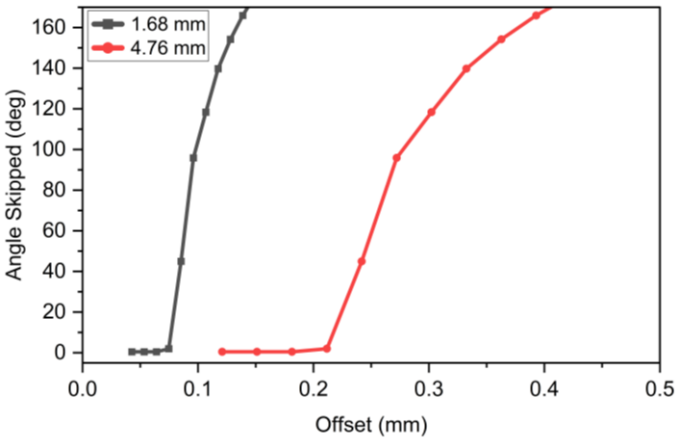

FIG. 12. Eccentricity tolerance curves for size-scaled HFCGs, based on a constant inductance of 100 μH and 17° Gurney Angle. The physically smaller generator (half-length, half-diameter) requires 3X more mechanical accuracy.

E. Eccentricity Effects Below Threshold

In an HFCG with eccentric misalignment between the armature and stator, prior to the onset of turn-skipping, the contact point velocity will still be affected. For the example of Fig. 13, the variation of the contact angle velocity is apparent. The contact angle being defined as the angle measured from the bottommost point of the stator helix, with each full turn corresponding to an additional 360 degrees. In this specific case, one would expect a spike in the *dI*/*dt* waveform at approximately 0.15 μs generator runtime due to the modulation of the *dL*/*dt* term in the lumped HFCG equation.

One notes that while these velocity variations do not directly cause flux loss as turn-skipping does, they may still contribute to some amount of additional flux loss as the flux diffusion ahead of the contact point is known to be related to the contact point velocity.[15] For a constant pitch, the effect typically occurs exactly 2π radians apart and is aptly termed as"2π clocking"[21]. In principle, this effect can be mitigated with perfect tolerance. However, achieving perfect tolerance is nearly impossible, so a remnant of the effect will pretty much always persist.

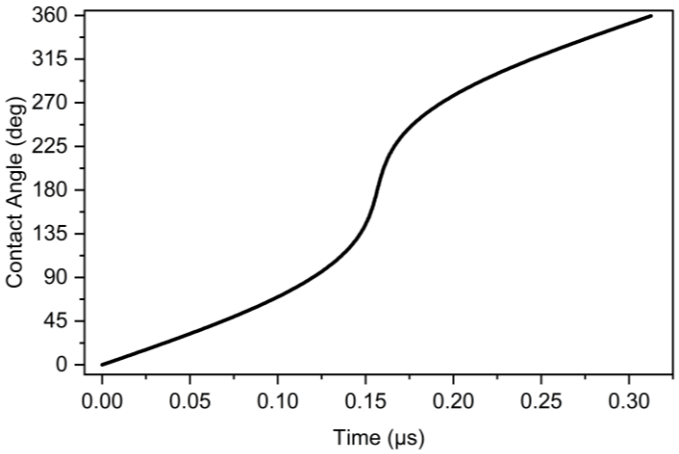

FIG. 13. Change in contact velocity over one turn of stator windings. Pitch: 2.5 mm, Detonation Velocity: 8 mm/μs, Gurney Angle: 17°, Eccentricity Offset: 0.102 mm.

Using the Blender simulation data as input, a behavioral LTSpice® model was developed. The LTspice® simulation for the single pitch HFCG is one that accounts for all the distinct phases during the generator's run time, like that of Young et. al.[12] To have a sufficient representation of the generator, one must include the following parameters as input, radius to the stator, length of the pitch section, the initial inductance of the coil, initial resistance of the coil, detonation velocity, gurney angle, and the flux loss parameter.[8, 17] At each distinct phase of generator operation, the lost volume is found as a function of time. The volume is normalized and multiplied by the initial inductance to obtain the inductance as a function of time, and in LTspice® is represented by a behavioral voltage source. This behavioral voltage source is used as an input into the behavioral model for the HFCG run.

To evaluate the impact of changing contact velocity on generator output, a small inductance change term is added, *dL/dt*, within the simulation to emulate a generator with a finite eccentricity:

$$\frac{dL}{dt} = \frac{dL}{d\phi} * \frac{d\phi}{dt} \tag{9}$$

with $dL/d\phi$ representing the differential inductance change (dL) per differential contact angle ($d\phi$), adjusted to match the experimental results found in Fryar et. al.[11] The parameter $d\phi/dt$ is the contact angle change per differential time, which was taken from the derivative of the Blender™ results, cf. Fig. 13.

Comparing the LTspice® simulation results with experimental data[11], see Fig. 14, one reasonably infers that the experimental *dI/dt* oscillations are suggestive of the presence of eccentric armature-stator alignment in the generator.

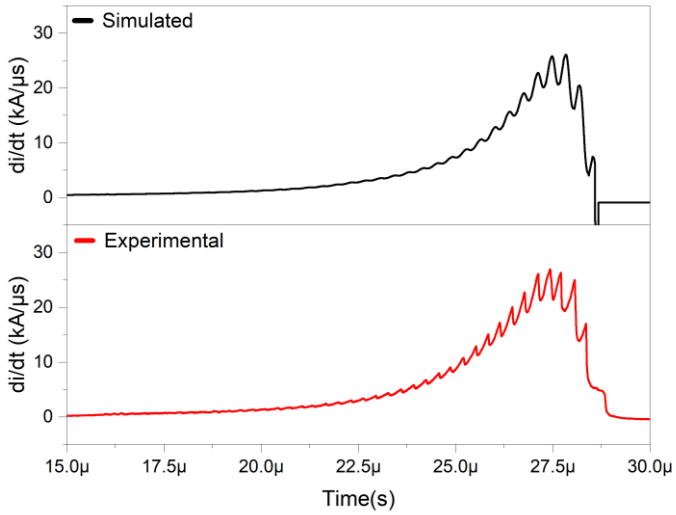

FIG. 14. Top - simulated *dI*/*dt* for a single-pitch HFCG, lumped circuit model. Modulation in the simulated *dI/dt* is due to the contact velocity modulation caused by finite eccentricity tolerances. Simulated with an eccentricity offset of 4.2 mm. Bottom - experimental waveform from Fryar el. al.[11]. Specifications for simulation and experiment: 50.8 mm helix diameter, 2.5 mm Pitch, 17° Gurney angle, 40 turns on the stator winding

It should be emphasized that, in the simulation, the changing contact velocity does not lead to flux loss in the form of partial turn skipping. In the experiment, it is presently unknown whether the mechanism responsible for the observed oscillations, presumed to be armature-stator misalignment, played a significant role in the overall flux loss. A beneficial extension to the LTSpice® simulation approach would be the capability to model flux loss through turn-skipping, in which case the simulation would be a helpful tool in estimating the impact of that particular loss mechanism on overall performance. Acknowledging that effort is generally best put into designing and fabricating generators that do not suffer from turn-skipping, the reality is that physical HFCGs experience multiple loss mechanisms. Loss due to armature-stator misalignment may constitute only a small fraction of the overall loss. If the HFCG designer had the benefit of this knowledge, they may choose to prioritize other loss mechanisms in design improvements. Here, we have shown that a pathway to this capability exists with this modeling approach.

F. Ellipticity

In the authors' experience, obtaining high-precision tolerance armature tubes is often one of the more challenging aspects of designing and fabricating smaller-scale HFCGs. Many factors of the armature construction and processing can introduce variables that are undesirable when testing HFCGs and maintaining high precision. Ellipticity in this case is defined as the armature not being perfectly round but taking on the shape of an ellipse, see Fig. 15.

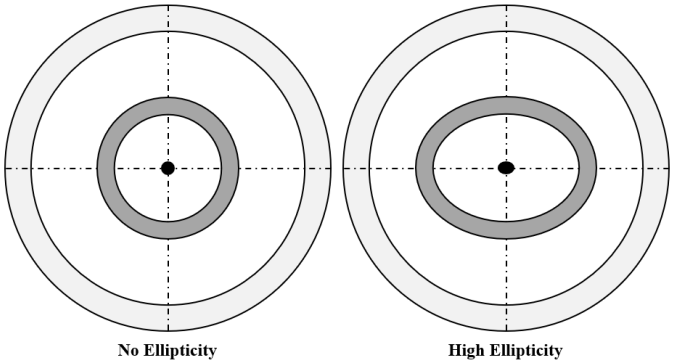

FIG. 15. Graphical depiction of (left) no armature ellipticity and (right) exaggerated armature ellipticity. The outer circle is depicted as the stator, with the inner darker being the armature.

Ellipticity in armatures can arise from many different factors, including wall thickness variations in the armature construction.[3] When an armature is not uniformly thick, the expanding armature can appear elliptical. Other factors that can cause deformations in the armature tube could be improper handling during post-manufacturing treatments and HFCG assembly. In the author's experience, this is a major obstacle and one which is difficult to control unless constructed in-house. Without specifying the detailed issue causing non-unform expansion, such as the mass and temper of the material[10], it is simply expressed as an azimuthal variation of the armature outer radius during expansion. Ellipticity offset is defined in this simulation as the difference between the minor and major radii of an ellipse, Side a and side b, respectively, in Fig. 16.

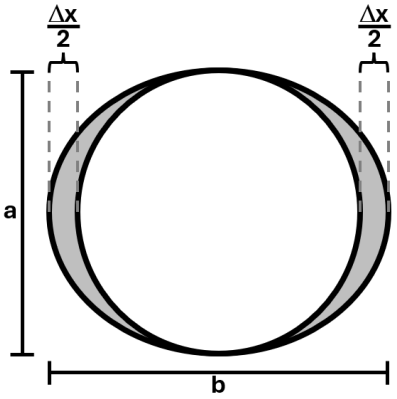

FIG. 16. Ellipticity offset definition. Both sides are offset by the specified amount divided by 2. The circle side a is maintained with an offset only being applied to side b. The offset is defined as the difference between side a and side b.

To generate this specific shape in Blender™, the technique with the truncated cone was utilized again as in the eccentricity armature creation. The simulation first creates the top radius based on the desired armature radius; this also adds the offsets defined in Fig. 16. It then creates the bottom radius a distance away, this distance is decided by the Gurney angle as well as making sure that it is wide enough to interact with all points on the stator winding. Once generated, the elliptical truncated cone follows the same technique as the eccentricity analysis cone.

As with the eccentricity analyses, a variation in Gurney angle shows that the allowable ellipticity tolerance increases with steeper angles. Also, as observed in the eccentricity analyses, varying pitch impacts allowable ellipticity tolerances, where increasing pitch results in tolerances that can be less strict. By normalizing the resultant analyses, in the same manner as carried out in the eccentricity analyses (i.e. by the Gurney angle and pitch) an ellipticity-driven universal scaling curve is generated, and is shown in Fig. 17,

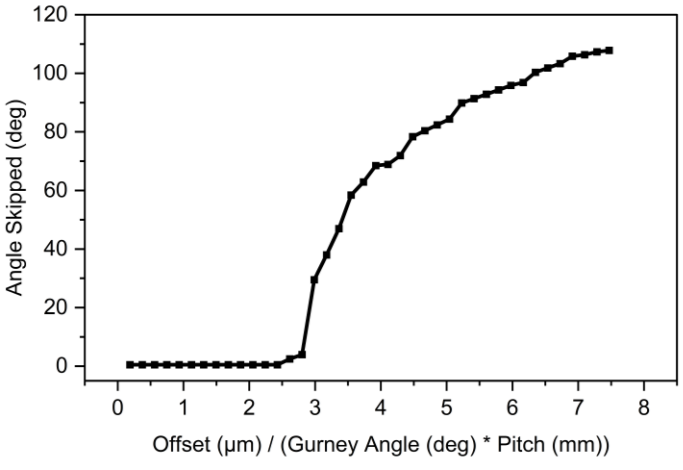

FIG. 17. Normalized Gurney angle and pitch ellipticity tolerance graph. Removal of common factors of pitch and Gurney angle results in a single curve. For a 17°, 2.5 mm pitch,

one reads an angle-skipping onset of ~ 120 μm based on the numerical value of ~2.8 on the abscissa.

This representation shows the direct relation between tolerance parameters and the effect of eccentricity tolerance variations. While this parameter needs to be heavily considered and mitigated when constructing HFCG's to prevent partial turn skipping, an understanding of the importance of pitch and Gurney angle when designing an HFCG is required. Designers need to understand the significance of choosing features that will provide the desired output results and will help mitigate partial turn-skipping when eccentricity and ellipticity tolerance parameters are not ideal. The relation between angle skipped and lost flux is beyond the scope of this paper and needs to be established for any specific generator design.

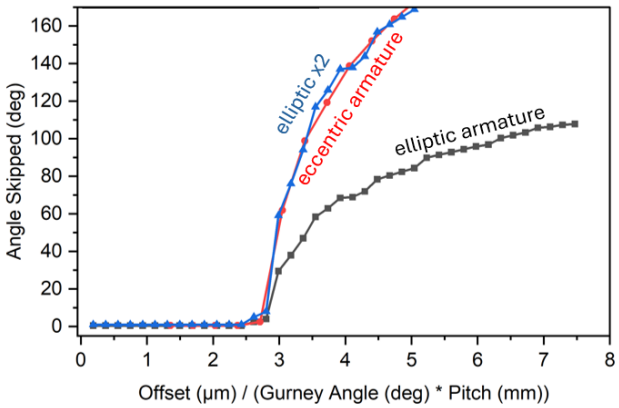

FIG. 18. Comparison between the normalized graphs of eccentricity and ellipticity tolerance deviations.

When comparing the normalized graphs for the eccentricity case and the elliptical armature analysis, different slope gradients are evident, see Fig. 18. After turn-skipping begins, the angle skipped due to eccentricity increases rapidly with offset, whereas ellipticity increases at about half that rate. Section B highlighted the differences between the two stator contact regions of the armature. In the eccentricity case, there is one high point for a given offset; in the ellipticity case, there are two. Thus, in the eccentricity case, a single skip is observed, whereas the ellipticity case exhibits two skips. By doubling the values for the angle skipped in the ellipticity case (see Fig. 18), the graphs align as expected. Minor variations in the graph are attributed to the simulation's resolution limits.

Similar to the eccentricity example, at a mechanical deviation too small to affect turn-skipping, a change in contact velocity is observed, see Fig. 19. Compared to the eccentricity case, the contact velocity for the ellipticity case has two distinct points at which the velocity increases in each turn. Analyzing the data in the experimental case in Fig. 14, one counts a total of 40 peaks, which was argued to be the result of the eccentricity offset revealing itself as "2π clocking". However, if it were to result from ellipticity tolerance, there would theoretically have to be 80 spikes in the *dI/dt* waveform since there would be two spikes seen per 2π cycle.

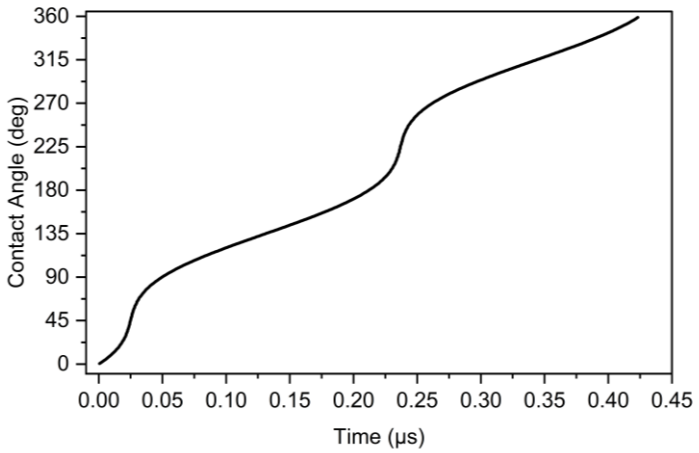

FIG. 19. Change in contact velocity over one turn of stator windings. Pitch: 2.5 mm, Detonation Velocity: 8 mm/μs, Gurney Angle: 17°, Ellipticity Offset: 0.102 mm.

More research is required to understand more deeply what contributes to mechanical tolerance defects in armatures. In this simulation, a constant, oblique uniformity of the armature was assumed. Defects related to ellipticity may occur in only portions of the armature due to handling and other postproduction events. Beyond the scope of the manuscript, a more in-depth analysis of the mechanical manufacturing tolerances would be needed to create an in-depth Blender simulation. That is, the Blender model can accommodate any expansion profile, no matter how complex. If a credible profile is established, potentially through hydrocode simulation, the presented model can assist in determining the likelihood of turn-skipping. Additionally, it can aid in developing tolerance requirements, even for complex combinations of mechanisms responsible for turn-skipping.

One such profile that could be examined in this context is the inclusion of stator defects. Given the unique generation method of the stator in Blender™, introducing defects by shifting points to mimic stator manufacturing flaws would provide insights into the resulting losses. In Blender™, each contact point on the stator winding is individually controlled, enabling the simulation of sudden changes in stator pitch, non-straightened wire, or variations in diameter by adjusting the stator points in simulation to replicate those of stators with manufacturing flaws or defects.

IV. Conclusion

A common source of generator performance loss is flux left behind in the generator due to partial turn skipping, typically rooted in mechanical non-uniformities incurred in a generator's construction. An advanced method for quantifying the effect of armature tolerances on the operation of HFCGs has been developed, surpassing traditional estimate equations. Results from the 3-D simulation quantified that the required eccentricity and ellipticity tolerances are heavily influenced by the armature's Gurney angle and the stator windings' pitch. A tolerance regime between the ideal case and turn skipping was identified, in which the contact point still continuously follows

the stator helix, however, with a distinct modulation of the contact point velocity.

The model identified a range of tolerances that can be applied to any single-pitch generator or a section of a multi-pitch generator. For instance, from the simulation results, an HFCG with a pitch of 5 mm and a Gurney angle of 15° requires tolerances in the armature – stator eccentricity better than 0.18 mm before partial turn-skipping occurs; beyond this point, the angle skipped on the stator progresses fast, potentially skipping multiple turns.

The simulation identifies the precise point when excessive eccentricity tolerances lead to partial turn-skipping. Additionally, it measures the periodic variation in contact point velocity due to finite tolerances in armature-stator eccentricity. This velocity modulation was then used as input for a lumped circuit HFCG model, establishing a connection between the eccentricity and the dominant characteristic of the experimental *dI/dt* waveform, rather than armature ellipticity.

V. Acknowledgment

This work was performed under the auspices of the U.S. Department of Energy by Lawrence Livermore National Laboratory under Contract DE-AC52-07NA27344.

References

[1] M. Lehr et al., “Helical explosive flux compression generator research at the Air Force research laboratory,” Digest of Technical Papers. 12th IEEE International Pulsed Power Conference. (Cat. No.99CH36358), Monterey, CA, USA, 1999, pp. 339-342 vol.1, doi: 10.1109/PPC.1999.825480.

[2] Neuber, A. (2005). Chapter 4.3 Criteria for prevention of armature “turn-skipping”. *Explosively Driven Pulsed Power: Helical Magnetic Flux Compression Generators* (pp. 109–120), Springer-Verlag Berlin Heidelberg.

[3] Pincosy P.A., Abe D.K., Chase, J.B. “Design of a High-Gain Flux-Compression Generator” In: Titov VM, Shvetsov GA (eds) *Megaguass Fields and Pulse Power Systems, Part 1* Nova Science Publishers, Commack, NY, 1990, pp 441-448

[4] Chernyshev V.K., Zharinov E.I., Kazokov S.A., Busin V.N., Vaneev V.E., Korotkov M.I. “Magnetic Flux Cutoffs in Helical Explosive Magnetic Generators” In: Folwer C.M., Caird R.S., Erickson D.J. (Eds) *Megaguass Technology and Pulsed Power Applications*, Plenum Press, New York 1987, pp. 455-469

[5] Neuber, A. (2005). “Chapter 4.2 Analysis of Armature/Stator Contact” In *Explosively Driven Pulsed Power: Helical Magnetic Flux Compression Generators* (pp. 97–109), Springer-Verlag Berlin Heidelberg.

[6] J. Rasty, X. Le, J. Dickens, A. Neuber and M. Kristiansen, “Design criteria for prevention of armature “turn-skipping” in helical magnetic flux compression generators,” Digest of Technical Papers. PPC-2003. 14th IEEE International Pulsed Power Conference (IEEE Cat. No.03CH37472), Dallas, TX, USA, 2003, pp. 1077-1080 Vol.2, doi: 10.1109/PPC.2003.1277998.

[7] P. Appelgren, N. Brenning, T. Hurtig, A. Larsson, B. M. Novac and S. E. Nyholm, “Modeling of a Small Helical Magnetic Flux-Compression Generator,” in IEEE Transactions on Plasma Science, vol. 36, no. 5, pp. 2662-2672, Oct. 2008, doi: 10.1109/TPS.2008.2003077.

[8] M. H. Khanzade, Y. Alinejad-Beromi and A. Shoulaie, “Calculation of Turn Skipping Losses in Helical Flux Compression Generators,” in IEEE Transactions on Plasma Science, vol. 40, no. 2, pp. 505-510, Feb. 2012, doi: 10.1109/TPS.2011.2175752.

[9] B. Novac, G. Șerban, and V. Zoița, “Armature Dynamics of Helical Magnetic Flux-Compression Generators,” TOME 34 1989 № 6, 1989. https://digilib.nipne.ro/colectii/files/original/1fdfd359dc53b36f17a31f707bf91f3bd80868e4.pdf#page=53

[10] Neuber, A. (2005). “Chapter 4.1 Armature Dynamics” In *Explosively Driven Pulsed Power: Helical Magnetic Flux Compression Generators* (pp. 53–97), Springer-Verlag Berlin Heidelberg.

[11] N. Fryar, K. Schriner, J. Stephens, J. Dickens, A. Young and A. A. Neuber, “Benchmarking the Suitability of Novec™ 4710 for Application in Flux Compression Generators,” in *IEEE Transactions on Plasma Science*, doi: 10.1109/TPS.2024.3382475.

[12] A. Young, A. Neuber and M. Kristiansen, “Modeling and Simulation of Simple Flux-Trapping FCGs Utilizing PSpice Software,” in IEEE Transactions on Plasma Science, vol. 38, no. 8, pp. 1794-1802, Aug. 2010, doi: 10.1109/TPS.2010.2048723.

[13] G. R. Olshausen, “Absolute formulae for the mutual inductance of coaxial solenoids,” *Phys. Rev.*, vol 31, no. 6, pp.617-636, Dec. 1910

[14] Kennedy, James E. “The gurney model of explosive output for driving metal.” In Explosive effects and applications, pp. 221-257. New York, NY: Springer New York, 1998.

[15] G. F. Kiuttu and J. B. Chase, “An armature-stator contact resistance model for explosively driven helical magnetic flux compression generators,” 2005 IEEE Pulsed Power Conference, Monterey, CA, 2005, pp. 435–440.

[16] Kennedy, James E. “Gurney energy of explosives: estimation of the velocity and impulse imparted to driven metals.” United States, 1972. Web. doi:10.2172/4656546.

[17] A. Young, A. Neuber and M. Kristiansen, “Modeling and Simulation of Simple Flux-Trapping FCGs Utilizing PSpice Software,” in *IEEE Transactions of Plasma Science*, vol. 38, no. 8, pp. 1794-1802, Aug. 2010, doi: 10.1109/TPS.2010.2048723

[18] F. T. Ulaby, Umberto Ravaioli, “Fundamentals of Applied Electromagnetics”, 7th ed. Boston, MA, USA: Pearson, 2015, p. 270.

[19] F. Herlach, "Explosive-driven energy generators with transformer coupling," *J. Phys. E: Sci. Instrum.*, vol. 12, no. 5, pp. 421–429, 1979, doi: 10.1088/0022-3735/12/5/021.

[20] P. V. Mironychev, "The calculation of cutoffs of magnetic flux in misaligned, helical, explosive-driven magnetic flux-compression generators," *High Temp.*, vol. 33, no. 4, pp. 628–635, 1995.

[21] J. W. Shearer, F. F. Abraham, C. M. Aplin, B. P. Benham, J. E. Faulkner, F. C. Ford, M. M. Hill, C. A. McDonald, W. H. Stephens, D. J. Steinberg, and J. R. Wilson, "Explosive-Driven Magnetic-Field Compression Generators," *J. Appl. Phys.*, vol. 39, no. 4, pp. 2102–2116, Mar. 1968, doi: 10.1063/1.1656496.

[22] N. Fryar *et al.*, "Comparative Analysis of Gas Insulation within a Simulated Helical Flux Compression Generator Geometry using Air, SF6, and Novec 4710," 2024. Available: https://www.osti.gov/servlets/purl/2375950.

[23] Blender Foundation, *Blender 4.0* [Computer software]. Available: https://www.blender.org, 2024.

[24] Python Software Foundation, *Python Language Reference*, version 3.11.7 [Online]. Available: https://www.python.org. 2024.